Theor Chem Acc (2014) 133:1493
DOI 10.1007/s00214-014-1493-6

REGULAR ARTICLE

Why edge inversion? Theoretical characterization of the bonding in the transition states for inversion in $F_nNH_{(3-n)}$ and $F_nPH_{(3-n)}$ ($n = 0$–3)

Lu T. Xu · Tyler Y. Takeshita · Thom H. Dunning Jr.

Received: 13 February 2014 / Accepted: 21 April 2014 / Published online: 14 May 2014

Abstract As first noted by Dixon et al. (J Am Chem Soc 108:2461–2462, 1986), heavily fluorinated pyramidal phosphorus compounds, e.g., $F_nPH_{(3-n)}$ with $n > 1$, invert through a T-shaped transition state (edge inversion) rather than the D_{3h}-like transition states (vertex inversion) found in the corresponding nitrogen compounds and less fluorinated phosphorus compounds. Subsequent studies by Dixon and coworkers established that this is a general phenomenon and has important chemical consequences. But what is the reason for the change in the structure of the transition state? Recent theoretical investigations have resulted in the discovery of a new type of chemical bond, the recoupled pair bond. In particular, it was found that recoupled pair bond dyads account for the hypervalency of the elements beyond the first row. In this paper, we show that recoupled pair bond dyads also account for the existence of the edge inversion pathway in heavily fluorinated phosphorus compounds and likely account for the presence of the lower energy inversion pathways in pyramidal compounds of other elements beyond the first row.

Keywords Edge inversion · Vertex inversion · Transition state · Recoupled pair bond · Recoupled pair bond dyad · Generalized valence bond (GVB) theory

Dedicated to the memory of Professor Isaiah Shavitt and published as part of the special collection of articles celebrating his many contributions.

L. T. Xu · T. Y. Takeshita · T. H. Dunning Jr. (✉)
Department of Chemistry, University of Illinois at Urbana-Champaign, 600 S Mathews Avenue, Urbana, IL 61801, USA
e-mail: thdjr@illinois.edu

L. T. Xu
e-mail: luxu1@illinois.edu

1 Introduction

The structures, energetics and properties of molecules formed from elements in the first row of the periodic table, Li to Ne, can be dramatically different from those formed from elements in the subsequent rows—the so-called *first-row anomaly*. The anomaly manifests itself in a number of ways, such as the inability of the first row p-block elements to form hypervalent species. N and P are an example of this anomaly: P is able to form hypervalent molecules such as PF_5 and PCl_5, while N only forms NF_3 and NCl_3. Another manifestation of the difference between N and P has drawn quite a bit of attention. The ground states of NH_3, NF_3, PH_3 and PF_3 are all pyramidal, as expected. However, NH_3, NF_3 and PH_3 invert through a transition state with D_{3h} symmetry, while the transition state for inversion in PF_3 is T-shaped with C_{2v} symmetry.

Investigations of the T-shaped pnictogen transition states for inversion were inspired by the experimental synthesis of the first molecule containing a T-shaped, tri-coordinated hypervalent phosphorous structure, 5-aza-2,8-dioxa-3,7-di-tert-butyl-l-phosphabicyclo[3.3.0]octa-3,6-diene (ADPO) [1, 2]. Another hypervalent 10-P-3 compound, an intermediate, was discovered by Lochschmidt and Schmidpeter at approximately the same time [3]. Following up on this discovery, Dixon and co-workers [4–8] explored the structures of the transition states for inversion in phosphorus compounds. They performed calculations on PH_3, FPH_2, F_2PH and PF_3 and found that F_2PH and PF_3 have T-shaped transition states while FPH_2 and PH_3 have D_{3h}–like transition states. They pointed out that when inversion occurs through a T-shaped structure, the lone pair orbital is in the molecular plane, not perpendicular to the plane as in the D_{3h}-like transition states. Inversion through a T-shaped transition state is referred to as *edge inversion*,

while inversion through a D_{3h}-like transition state is referred to as *vertex inversion*.

Arduengo, Dixon and Roe experimentally verified the edge inversion mechanism in a bi-cyclo[3.3.0] octane ring system that is a saturated analog of ADPO by measuring the barrier to inversion at the tricoordinated phosphorous atom [5]. Although ADPO contains a T-shaped phosphorus structure in its ground state, its saturated analog contains a pyramidal phosphorus structure in its ground state and a T-shaped phosphorus structure in its transition state. They argued that the conjugated π system of ADPO stabilizes the T-shaped structure while the saturated analog of ADPO is not so stabilized. The electronic structure of all of these molecules can be easily understood once one recognizes the ability of phosphorous to form both covalent and recoupled pair bonds in simple tricoordinated molecules such as PF_3 [9], as will be shown in this paper.

Although edge inversion has been well established for pyramidal molecules with central atoms beyond the first row and with electronegative ligands, the reason for the difference in inversion pathway upon fluorination has been the subject of some debate. Both perturbation molecular orbital arguments involving the HOMO–LUMO gap [10] as well as pseudo-Jahn–Teller effects [11] have been used to rationalize the T-shaped transition state structures. Woon and Dunning, on the other hand, noted that the two axial bonds in the transition state for inversion in PF_3 closely resemble those in the $PF_2(A^2\Pi)$ state, which has a recoupled pair bond dyad, and concluded that the ability of the P atom to form a very stable recoupled pair bond dyad is the source of this anomaly [9]. In fact, the formation of recoupled pair bonds is the basis for the bonding in hypervalent molecules, as shown in studies on SF_n [12], PF_n [9], ClF_n [13] and a number of related compounds. The T-shaped transition state for inversion of PF_3 should, in fact, be considered hypervalent, even though it is tricoordinated, because it possesses one of the hallmarks of hypervalent compounds—a recoupled pair bond dyad.

In the present study, we systematically investigated the ground and transition states for inversion of NH_3, PH_3 and their F substituents, $F_nNH_{(3-n)}$ and $F_nPH_{(3-n)}$ ($n = 1$–3), and show that other than PF_3, F_2PH is the only species with a T-shaped transition state. Accurate predictions of the structures and energies of the $F_nNH_{(3-n)}$ and $F_nPH_{(3-n)}$ ($n = 0$–3) species were obtained by using coupled cluster methods [14–17] with large correlation consistent basis sets [18–21]. We then used generalized valence bond (GVB) theory [22, 23] to obtain insights into the nature of the bonding in these molecules and explain the similarities and differences in the structural and energetic trends of the N and P species.

The layout of the paper is as follows: Sect. 2 describes the computational methods we used for this study, including a brief overview of GVB theory; Sect. 3 presents the optimized geometries and energetics for the ground and transition states of $F_nNH_{(3-n)}$ and $F_nPH_{(3-n)}$, proposes the three major questions we need to answer, analyzes the GVB wave functions of related atoms and molecules, discusses the role recoupled pair bonding plays in the transition states and answers the questions raised; and finally, we summarize our findings in Sect. 4.

2 Computational methods

The calculations presented in this study were performed with the Molpro suite of quantum chemical programs (version 2008.1 and 2010.1) [24]. In order to provide accurate geometries and energetics, the structures, energies and frequencies of the $F_nNH_{(3-n)}$ and $F_nPH_{(3-n)}$ molecules were determined with single-reference restricted singles and doubles coupled cluster theory with perturbative triples [CCSD(T)] [14–17]. For geometry optimizations and energies, augmented correlation consistent basis sets of quadruple zeta quality (aug-cc-pVQZ) were used for the first row atoms (H, N and F), and the corresponding d-function augmented set [aug-cc-pV(Q + *d*)*Z*] was used for the second row P atom. For frequency calculations, aug-cc-pVTZ basis sets were used for the first row atoms and an aug-cc-pV(T + *d*)*Z* basis set was used for the P atom [18–21]. The frequency calculations were performed at geometries optimized using the same basis sets. The shorthand notation AVXZ (X = T, Q) will be used to represent the sets of a specific quality (including the extra d-function on the P atom). The frequency calculations enabled us to conclusively identify the ground states (all real frequencies) and transition states (one imaginary frequency) for all of the species.

The inversion barrier for each molecule is calculated as the difference between the electronic energy of the transition state and the ground state, i.e., it does not include the zero point energy correction. We did this to focus on the effect of the changes in the electronic structure of the molecules upon inversion; the reader can easily correct these numbers using the vibrational frequencies given in the tables. Energies are quoted with two significant figures after the decimal place for comparison with other theoretical calculations.

Multireference configuration interaction (MRCI) calculations based on valence complete active space self-consistent field (CASSCF) wave functions with the quadruples corrections (+Q) [25–30] were used to determine the excitation energies of the N and P atoms using the AVQZ basis set.

To characterize the nature of the bonding in the $F_nNH_{(3-n)}$ and $F_nPH_{(3-n)}$ species, we used the generalized

valence bond (GVB) method [22, 23]. The GVB wave function is well suited to analysis of the bonding in molecules as it describes bond-breaking processes properly. The GVB wave function is also inherently more accurate than the Hartree–Fock (HF) wave function, including the most important non-dynamical correlation effects represented in a valence CASSCF wave function. At the same time, the GVB wave function is concise, offering a clear physical picture of the electronic structure of a molecule that is readily connected with those of the atoms or fragments of which it is composed.

In the GVB framework, a covalent bond is formed by singlet coupling two electrons in a pair of overlapping, singly occupied GVB orbitals concentrated on the two atoms involved in the bond. A recoupled pair bond, on the other hand, results from a two-center, three-electron interaction. Nevertheless, it is also easily described in GVB theory because each electron has its own orbital [31]. The recoupled pair bond dyad, which is of particular interest here, is simply two singlet-coupled bonding pairs—one from the original recoupled pair bond and the other from a covalent bond formed with the electron left over from forming the recoupled pair bond. The remarkable stability of the recoupled pair bond dyad is a direct result of the ionicity of these two bonds—a dyad is only found when the two ligands are very ionic [32, 33]. The GVB orbitals, orbital overlaps and spin coupling functions provide a concise picture of the electronic structure of the molecule. The fully variational GVB method is equivalent to the spin-coupled VB method [34], and the CASVB [35–37] program implemented in Molpro was used to perform the calculations with the AVQZ basis sets.

The GVB/spin-coupled VB wave function for a molecular system of n_a active electrons with total spin S and projection M is:

$$\Psi_{\mathrm{GVB}} = \hat{a}\phi_{d1}\phi_{d1}\phi_{d2}\phi_{d2}\ldots\phi_{dn_d}\phi_{dn_d}\varphi_{a1}\varphi_{a2}\ldots\varphi_{an_a}\alpha\beta\alpha\beta\ldots\alpha\beta\Theta^{n_a}_{S,M}. \quad (1)$$

In the above equation, $\hat{a}$ is the antisymmetrizer; the set of orbitals, $\{\phi_{di}\}$, are the set of n_d doubly occupied core and valence orbitals, and the set of orbitals, $\{\varphi_{ai}\}$, are the set of n_a singly occupied active valence orbitals. The total number of electrons is $N_e = 2n_d + n_a$. The doubly occupied valence orbitals do not directly participate in bonding, although, as we shall see, they can affect which type of bonds are formed. The active orbitals are distinct, singly occupied and non-orthogonal orbitals. The spatial product of orbitals in Eq. (1) is multiplied by a product of $\alpha\beta$ spin functions associated with the doubly occupied orbitals times a spin function, $\Theta^{n_a}_{S,M}$, for the electrons in the active orbitals. This spin function is a linear combination of spin eigenfunctions, also known as spin basis functions, which represent the unique ways in which the spins of the n_a electrons in the active orbitals can be coupled to give a total spin of S. Kotani spin functions [38] were used in our study. The Kotani functions are orthogonal to each other, and, therefore, the contribution of each spin function to the total GVB wave function, the weight w_k, is simply the square of its coefficient.

We found that one of the spin eigenfunctions was dominant for all of the molecular systems that we studied here, and it is the perfect pairing (PP) function:

$$\Theta^{n_a}_{S,M,\mathrm{PP}} = \frac{(\alpha\beta-\beta\alpha)}{\sqrt{2}}\frac{(\alpha\beta-\beta\alpha)}{\sqrt{2}}\cdots\frac{(\alpha\beta-\beta\alpha)}{\sqrt{2}} \quad (2)$$

As shown in Eq. (2), the perfect pairing spin function singlet couples all of the active electrons into electron pairs. A pair of singlet-coupled orbitals can describe a lone pair, in which case the orbitals are highly overlapping and concentrated on one atom. Or the orbital pair can describe a bond if the orbitals are overlapping and concentrated on two atoms. The GVB calculations for the states reported in this paper are all 6-in-6 calculations, i.e., there are six active electrons in six GVB orbitals. All spin functions were included in the calculations, although, as noted, the PP spin function was always dominant ($w_{\mathrm{PP}} = 0.91$–$0.99+$). This means that there are three pairs of singlet-coupled orbitals, or, since we kept the lone pair orbitals doubly occupied in all calculations, three bonds in both the ground and transition states of the $F_nNH_{(3-n)}$ and $F_nPH_{(3-n)}$ molecules.

3 Results and discussion

3.1 Similarities and differences in the $F_nNH_{(n-3)}$ and $F_nPH_{(3-n)}$ ($n = 0$–3) ground states and transition states for inversion

3.1.1 Molecular structures

The optimized structures and geometrical parameters of the ground state (GS, X^1A_1) and transition state (TS, $^1A_1$) of all of the $F_nNH_{(3-n)}$ and $F_nPH_{(3-n)}$ ($n = 0$–3) molecules are tabulated in Tables 1, 2, 3 and 4 and illustrated in Fig. 1. The ground states of $F_nNH_{(3-n)}$ and $F_nPH_{(3-n)}$ are pyramidal with the singly occupied 1s orbitals of H(^{2}S) and the singly occupied 2p orbitals of F(^{2}P) forming normal 2-electron, 2-center covalent bonds with the three singly occupied 2p and 3p orbitals on N(^{4}S) and P(^{4}S), respectively. However, the inversion transition states fall into two different structural categories. NH_3, NF_3 and PH_3 have planar transition states with D_{3h} symmetry ($\theta_{\mathrm{XYX}} = 120°$). The transition states of FNH_2 and FPH_2 are planar with C_{2v} symmetry and similar bond angles: $\theta_{\mathrm{HNF}} = 114.0°$ and

Table 1 The geometries, frequencies and total energies for the ground states (GS) of the $F_nNH_{(3-n)}$ ($n = 0$–3) molecules from CCSD(T) calculations with the indicated basis sets

		R_{NH}	R_{NF}	θ_{HNH}	θ_{FNH}	θ_{FNF}	ω_1	ω_2	ω_3	ω_4	ω_5	ω_6	E
NH_3	AVTZ	1.015		106.4			1,063	1,672	1,672	3,463	3,592	3,592	−56.480527
	AVQZ	1.013		106.5			1,059	1,674	1,674	3,476	3,606	3,607	−56.495733
FNH_2	AVTZ	1.021	1.433	104.8	101.1		927	1,270	1,341	1,623	3,410	3,507	−155.541406
	AVQZ	1.019	1.426	105.0	101.3								−155.582143
F_2NH	AVTZ	1.027	1.400		99.8	103.0	504	910	992	1,343	1,467	3,367	−254.621481
	AVQZ	1.025	1.394		100.0	103.1							−254.687975
NF_3	AVTZ	1.375				101.7	498	498	654	924	924	1,045	−353.714384
	AVQZ	1.369				101.8							−353.806789

Distances are in Å, angles in degrees, frequencies in cm^{-1} and energies in Hartrees

Table 2 The geometries, frequencies and total energies for the inversion transition states (TS) of the $F_nNH_{(3-n)}$ ($n = 0$–3) molecules from CCSD(T) calculations with the indicated basis sets

		R_{NH}	R_{NF}	θ_{HNH}	θ_{FNH}	θ_{FNF}	ω_1	ω_2	ω_3	ω_4	ω_5	ω_i	E
NH_3	AVTZ	0.998		120.0			1,582	1,582	3,626	3,837	3,837	868	−54.471739
	AVQZ	0.996		120.0			1,582	1,583	3,633	3,846	3,847	850	−56.487226
FNH_2	AVTZ	0.996	1.385	132.0	114.0		1,078	1,189	1,552	3,674	3,898	1,148	−155.515766
	AVQZ	0.995	1.381	132.0	114.0								−155.557208
F_2NH	AVTZ	0.998	1.352		123.7	112.6	493	1,092	1,171	1,336	3,786	1,373	−254.559030
	AVQZ	0.997	1.348		123.7	112.6							−254.626575
NF_3	AVTZ		1.343			120.0	420	420	802	1,313	1,313	1,192	−353.581416
	AVQZ		1.338			120.0							−353.674851

Distances are in Å, angles in degrees, frequencies in cm^{-1} and energies in Hartrees. ω_i denotes the imaginary frequency associated with transition state motion

Table 3 The geometries, frequencies and total energies for the ground states (GS) of the $F_nPH_{(3-n)}$ ($n = 0$–3) molecules from CCSD(T) calculations with the indicated basis sets

		R_{PH}	R_{PF}	θ_{HPH}	θ_{FPH}	θ_{FPF}	ω_1	ω_2	ω_3	ω_4	ω_5	ω_6	E
PH_3	AVTZ	1.417		93.5			1,013	1,143	1,143	2,409	2,416	2,416	−342.699014
	AVQZ	1.415		93.6			1,012	1,143	1,143	2,421	2,429	2,429	−342.710887
FPH_2	AVTZ	1.420	1.613	92.1	97.7		809	927	975	1,138	2,378	2,383	−441.866170
	AVQZ	1.419	1.607	92.1	97.8								−441.905727
F_2PH	AVTZ	1.424	1.591		95.6	98.8	354	841	848	971	1,023	2,344	−541.056075
	AVQZ	1.423	1.585		95.7	98.9							−541.123513
PF_3	AVTZ		1.572			97.4	344	344	484	862	862	894	−640.266595
	AVQZ		1.567			97.5							−640.362060

Distances are in Å, angles in degrees, frequencies in cm^{-1} and energies in Hartrees

$\theta_{HPF} = 114.9°$. The transition state of F_2NH is also of C_{2v} symmetry with θ_{HNF} at 123.7°. These latter three C_{2v} transition states are, in fact, D_{3h}-like and fall into the same structural category as NH_3, NF_3 and PH_3.

The transition states for F_2PH and PF_3, on the other hand, are outliers. In the transition state for inversion of F_2PH, the central P atom and two of the F atoms, the axial F atoms, lie almost on a straight line with $\theta_{FPF} = 169.8°$ and $\theta_{HPF} = 84.9°$. This quasi-linear structure is also present in PF_3, where the FPF axial angle is 176.0° and the angle between the axial and equatorial F atom is 88.0°. These two transition states are referred to as T-shaped transition states as first characterized by Dixon and coworkers [4–8] and are referred to as *edge* transition states in contrast to the transition states for the other six $F_nNH_{(3-n)}$ and $F_nPH_{(3-n)}$ molecules, which are referred to as *vertex* transition states.

Table 4 The geometries, frequencies and total energies for the inversion transition states (TS) of the $F_nPH_{(3-n)}$ ($n = 0$–3) molecules from CCSD(T) calculations with the indicated basis sets

		R_{PH}	R_{PF}	θ_{HPH}	θ_{FPH}	θ_{FPF}	ω_1	ω_2	ω_3	ω_4	ω_5	ω_i	E
PH_3	AVTZ	1.380		120.0			1,017	1,017	2,597	2,676	2,676	1,098	−342.645628
	AVQZ	1.379		120.0			1,023	1,023	2,605	2,684	2,684	1,096	−342.657904
FPH_2	AVTZ	1.376	1.590	130.2	114.9		719	871	1,001	2,626	2,712	1,255	−441.785348
	AVQZ	1.375	1.585	130.2	114.9								−441.825182
F_2PH	AVTZ	1.414	1.655(ax)		84.9	169.8	422	582	740	1,319	2,404	348	−540.975049
	AVQZ	1.413	1.649(ax)		84.9	169.8							−541.040581
PF_3	AVTZ		1.566(eq)			88.0	389	503	578	769	888	312	−640.182433
			1.635(ax)										
	AVQZ		1.561(eq)			88.0							−640.276004
			1.630(ax)										

Distances are in Å, angles in degrees, frequencies in cm^{-1} and energies in Hartrees. ω_i denotes the imaginary frequency associated with transition state motion. The labels, "eq" and "ax," refer to the equatorial and axial bonds in F_2PH and PF_3

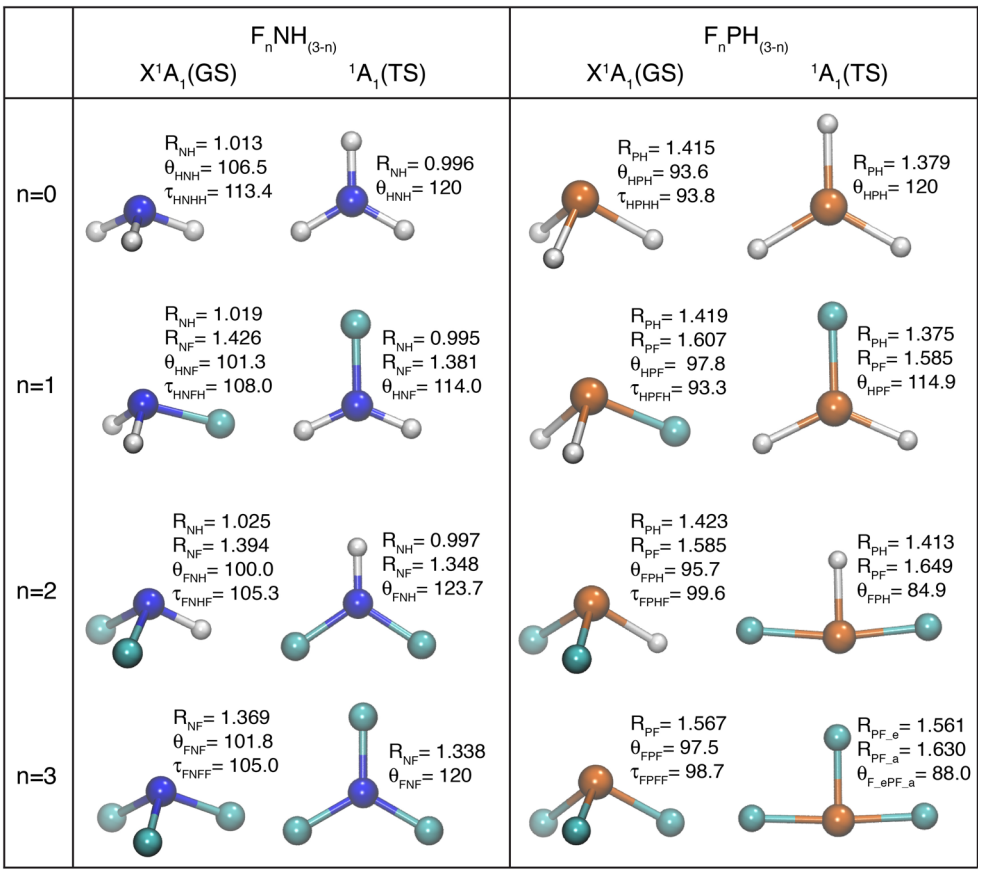

Fig. 1 Optimized geometries of the $F_nNH_{(3-n)}$ and $F_nPH_{(3-n)}$ ($n = 0$–3) ground states (GS, X^1A_1) and the transition states for inversion (TS, $^1A_1$) obtained from CCSD(T)/AVQZ calculations. Bond distances are in Å and bond angles in degree. θ corresponds to bond angle and τ corresponds to dihedral angle. N is color coded in *blue*, P in rusty *orange*, F in cyan and H in *gray*

The above observations lead to **Question #1**: What is the cause of the differences in the structures of the transition states of (F_2NH, F_2PH) and (NF_3, PF_3), as well as those of (PH_3, FPH_2) and (F_2PH, PF_3)?

Besides the obvious structural differences, a closer examination of the bond distances shows that for all of the molecules that have D_{3h} or D_{3h}-like transition states, i.e., NH_3, FNH_2, F_2NH_3, NF_3, PH_3 and FPH_2, the bond lengths in the transition states are all shorter than the ground state bond lengths. However, the differences in the bond lengths in F_2PH and PF_3 do not follow the same simple pattern. For F_2PH, the PH bond distance is slightly shorter ($\Delta = -0.010$ Å) and the PF bond distances are significantly longer ($\Delta = +0.064$ Å) in the transition state than in the

Table 5 The changes in the bond lengths, ΔR, in $F_nNH_{(3-n)}$ and $F_nPH_{(3-n)}$ ($n = 0$–3), between the ground states (GS) and the inversion transition states (TS): $\Delta R = R(\text{TS}) - R(\text{GS})$, in Å

n	ΔR_{NH}(Å)	ΔR_{NF}(Å)	ΔR_{PH}(Å)	ΔR_{PF}(Å)	ΔR_{PF}(Å)	
					Axial	Equatorial
0	−0.017 (−1.7)		−0.036 (−2.5)			
1	−0.024 (−2.4)	−0.045 (−3.2)	−0.044 (−3.1)	−0.022 (−1.4)		
2	−0.028 (−2.7)	−0.046 (−3.3)	−0.010 (−0.7)		0.064 (4.0)	
3		−0.031 (−2.3)			0.063 (4.0)	−0.006 (−0.4)

The percentage change with respect to the bond distance in the ground state is given in parentheses

ground state. For PF_3, the transition state has two types of PF bonds. The two axial PF bonds are much longer ($\Delta = +0.063$ Å) than the ground state PF bond, and the equatorial PF bond is slightly shorter ($\Delta = -0.006$ Å) than the ground state PF bond.

Table 5 summarizes the bond distance changes between the ground state and transition state of all eight molecules. The percentage changes with respect to the bond lengths in the ground state are also listed (in parentheses). The percentage change for molecules in the D_{3h}-like category ranges from −1.4 % to −3.1 %. On the other hand, the percentage change for the PH bond in F_2PH is only −0.7 %, which is very close to the −0.4 % change for the equatorial PF bond in F_2PF. The percentage change for the axial PF bonds when $n = 2$ and $n = 3$ is 4.0 %, which is larger than any of the differences in the other molecules. These data lead to **Question #2**: Why do the bond distances of the D_{3h}-like transition states decrease and those of the T-shaped transition states behave very differently?

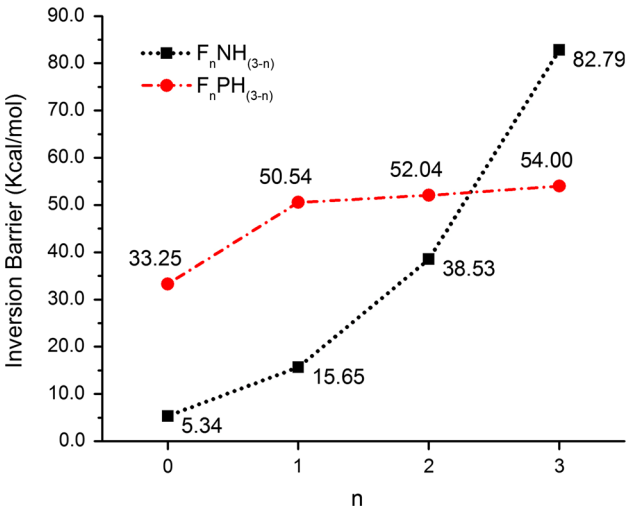

Fig. 2 Computed inversion barriers for $F_nNH_{(3-n)}$ and $F_nPH_{(3-n)}$ ($n = 0$–3) from CCSD(T)/AVQZ calculations. The inversion barrier is the electronic energy difference between the transition state and the ground state for each molecule without zero-point energy correction

3.1.2 Inversion barrier

Here, as noted in Sect. 2, the inversion barrier is defined as the difference in the electronic energies of the transition state and the ground state, i.e., we ignore differences in the zero-point energies even though vibrational frequencies are reported, because we want to focus on the variations in the barriers caused by the changes in the electronic structure of the molecules. Figure 2 shows the plot of the inversion barrier with respect to n, the number of F atoms in the molecule. When N is the central atom, the barrier height increases monotonically from 5.34 to 82.79 kcal/mol as n increases from 0 to 3. The rate of increase increases with n as well, essentially doubling with each additional F atom: 10.31 kcal/mol from $n = 0$–1, 22.88 kcal/mol from $n = 1$–2 and 44.26 kcal/mol from $n = 2$–3. When P is the central atom, the barrier height increases from 33.25 kcal/mol to just 54.00 kcal/mol as n increases from 0 to 3. The rate of increase is 17.29 kcal/mol from $n = 0$–1, but only 1.50 kcal/mol from $n = 1$–2 and 1.96 kcal/mol from $n = 2$–3. Thus, from $n = 1$–3, the change in the height of the inversion barrier is vastly different in the N series than in the P series: The total increase in the barrier height for $F_nNH_{(3-n)}$ is 77.45 kcal/mol while the barrier height increase for $F_nPH_{(3-n)}$ is less than a third of that, 20.75 kcal/mol. So **Question #3** is: Why does the barrier change very little from $n = 1$–3 in the $F_nPH_{(3-n)}$ series, instead of increasing dramatically like the $F_nNH_{(3-n)}$ series does?

As an aside, we did locate higher lying "transition states" in both F_2PH and PF_3. The geometry of the D_{3h}-like transition state in F_2PH is $R_{PH} = 1.375$ Å, $R_{PF} = 1.571$ Å and $\theta_{HPF} = 124.8°$. This structure lies 32.72 kcal/mol above the lower transition state, at 84.76 kcal/mol. It is a true transition state with only one imaginary frequency: 1,158.2i cm^{-1} (because of its high energy, we did not follow the reaction path from this transition state to see where it led). When PF_3 is constrained to have a D_{3h} structure, $R_{PF} = 1.633$ Å. The D_{3h} structure lies 33.12 kcal/mol higher than the T-shaped transition state

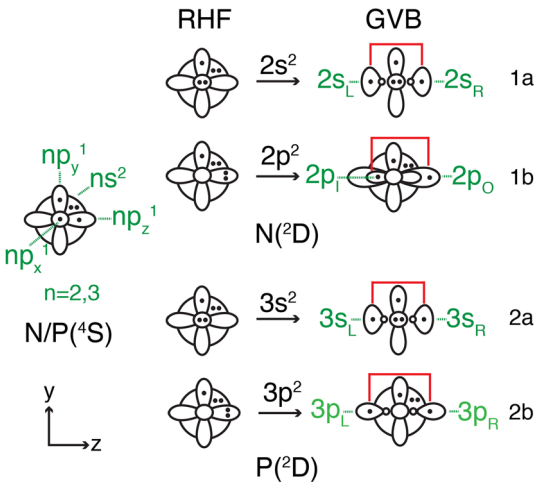

Fig. 3 HF and GVB diagrams for N and P atoms; $n = 2$ for N and $n = 3$ for P atom. The subscripts "L", "R", "I" and "O" represent left, right, inner and outer. The electrons in orbital pairs connected with a red line are singlet coupled

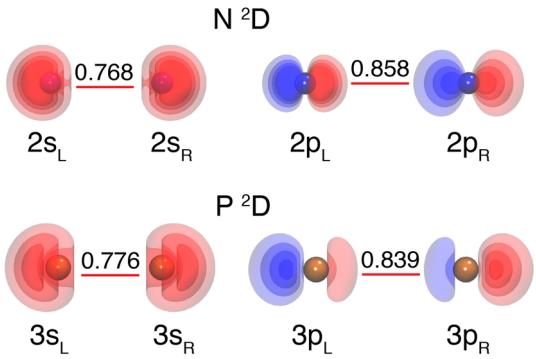

Fig. 4 GVB orbitals and overlaps for the N(^{2}D) and P(^{2}D) states. A *red line* means that the electrons in these singly occupied orbitals are singlet coupled; the values of the orbital overlaps are given above the line. Contours are ±0.10, ±0.15, ±0.20 and ±0.25. *Red contour* represents positive, and *blue contour* represents negative orbital phase

and 87.12 kcal/mol above the ground state PF_3. However, this configuration has three imaginary frequencies ($2 \times 214i$, $596i$ cm^{-1}) and therefore is not a true transition state.

3.2 p-Recoupled pair bonding in F_2PH and PF_3 and s-recoupled pair bonding in the other molecules

In the last section, we posed three questions. In this section, we show that the answers to all of these questions center on the ability of the P atom to form recoupled pair bonds with F and, more specifically, p-recoupled pair bond dyads with two F atoms. In molecules other than F_2PH and PF_3, the inversion transition states involve formation of s-recoupled pair bond dyads.

3.2.1 GVB description of the N and P atoms

In order to understand the differences between $F_nNH_{(3-n)}$ and $F_nPH_{(3-n)}$ ($n = 0$–3), we need to understand the differences between the central atoms in these molecules. Figure 3 presents the GVB orbital diagrams for the ground and low-lying excited states of the N and P atoms. The diagrams represent the valence electrons and orbitals. The ground states of the N and P atoms are ^{4}S states with three singly occupied valence p orbitals in each atom. In the N/P(^{4}S) diagram, the big circle represents the valence s orbital, the small circle represents the out-of-plane p_x orbital, and the two dumbbell shapes represent the two in-plane (p_y, p_z) orbitals. The dots represent electron occupations. The ground states of $F_nNH_{(3-n)}$ and $F_nPH_{(3-n)}$ ($n = 0$–3) have three normal covalent bonds formed with the electrons in these three singly occupied p orbitals. The pyramidal structures of these molecules are a natural result of the orientations of the three p orbitals in the atom.

Although the connection of the ground states of the N and P atoms with the ground states of the $F_nNH_{(3-n)}$ and $F_nPH_{(3-n)}$ molecules is straightforward, the transition states do not correlate with the ground state atoms. Rather, they correlate with the first excited (^{2}D) states of the atoms. In this state, one electron from a p orbital is excited into one of the other p orbitals with the original p orbital no longer occupied in the configuration (this is schematically represented by the configuration $s^2p_x^2p_y^1$ or $s^2p_z^2p_y^1$ in Fig. 3). Now, the atoms can form both covalent bonds (with the singly occupied p_y orbital) as well as recoupled pair bonds and recoupled pair bond dyads (with the s^2 or p^2 lone pairs). The calculated excitation energy from the ^{4}S state to the ^{2}D state is 55.33 kcal/mol for the N atom and 32.23 kcal/mol for the P atom (MRCI + Q/AVQZ); these numbers are to be compared to 54.97 and 32.48 kcal/mol from the NIST Atomic Spectra Tables [39]. Because of this energetic difference, recoupled pair bonds and recoupled pair bond dyads in P will lie at much lower energies than in N.

As noted above, there are two doubly occupied orbitals in the ^{2}D state, i.e., $2s^2$ and $2p^2$ for N and $3s^2$ and $3p^2$ for P atom. Although these orbitals are doubly occupied in the HF wave function, in the GVB wave function s^2 and p^2 lone pairs are each described by two singly occupied, non-orthogonal lobe orbitals. Figure 4 shows the s and p GVB lobe orbitals for the N(^{2}D) and P(^{2}D) states. The s lobe orbitals of both atoms are very similar in shape and orientation, although the P orbitals are more diffuse and span a larger spatial region. The s lobe orbitals are well separated spatially, residing on opposite sides of the central atom, and have overlaps of only 0.768 (N) and 0.776 (P); we refer to them as the s_L and s_R lobe orbitals. In the GVB orbital diagrams 1a and 2a in Fig. 3, the s_L and s_R lobe

orbitals are connected with a red line, representing the fact that they are singlet coupled.

On the other hand, the 2p lobe orbitals of N(^{2}D) and the 3p lobe orbitals of P(^{2}D) are very different. Both 2p lobe orbitals on the N(^{2}D) state look like p orbitals, one tighter than the original $2p_z$ orbital and the other one more diffuse. They lie in the same spatial region, and we refer to them as inner and outer lobe orbitals, $2p_I$ and $2p_O$. In the N(^{2}D) GVB orbital diagram 1b in Fig. 3, these orbitals are represented with two dumbbell shapes, one inside of the other with a red line connecting them. The 3p lobe orbitals of P(^{2}D), on the other hand, are distorted $3p_z$ orbitals, with one more concentrated on the left side of the P atom and the other more concentrated on the right side; they have an overlap of 0.839 and are referred to as $3p_L$ and $3p_R$ lobe orbitals. In diagram 2b in Fig. 3, they are represented with two half-dumbbell shapes connected with a red line.

Both of the lone pairs on the N and P atoms are potentially available for recoupling to form bonds. However, the ease with which a lone pair can be recoupled is dependent on two factors: (1) the spatial orientation of the lobe orbitals and (2) the overlap of the orbitals. To form a strong recoupled pair bond or recoupled pair bond dyad, the lobe orbitals must be localized in different spatial regions and the overlap of the lone pair orbitals must be significantly less than one (the smaller, the better). It also helps if the ligand is very electronegative, because this will reduce the Pauli exchange-repulsion between the bonds (or between the bond and the electron in the left over orbital) formed by recoupling the lone pair [31].

As noted above, the N and P s_L and s_R orbitals are spatially well separated and their overlaps, 0.768 (N) and 0.776 (P), are similar. So, s-recoupled pair bonds can be formed in both N and P. The overlap between the N $2p_I$ and $2p_O$ orbitals (0.858) is slightly larger than that between the P $3p_L$ and $3p_R$ orbitals (0.839), and both overlaps are much larger than the overlaps between the ($2s_L$, $2s_R$) and ($3s_L$, $3s_R$) lobe orbitals. But, more importantly, the $2p_I$ and $2p_O$ orbitals occupy essentially the same spatial region, while the $3p_L$ and $3p_R$ orbitals are spatially separated. Therefore, it is far more favorable for P to participate in p-recoupled pair bonding than N. However, the ($3p_L$, $3p_R$) orbitals of the P atom are not as spatially separated as the ($3s_L$, $3s_R$) orbitals, so it will be more difficult to form recoupled bonds with the 3p lone pair than with the 3s lone pair.

From the GVB orbital diagram of the P(^{2}D) state in Fig. 3, one can easily see that three strong bonds can be formed: with the singly occupied ($3s_L$, $3s_R$, $3p_y$) orbitals in 2a and the singly occupied ($3p_L$, $3p_R$, $3p_y$) orbitals in 2b. In 2a, the remaining lone pair is an out-of-plane $3p_x$ lone pair, and in 2b, it is an in-plane 3s pair. As will be demonstrated and discussed in Sects. 3.2.2 and 3.2.3, with 2a, the resulting structures of the transition states correspond to that of the D_{3h}-like structures, which have an out-of-plane lone pair. With 2b, the resulting structures will be those of the T-shaped transition states for inversion with an in-plane lone pair. Since the lobe orbitals in 1a, 2a and 2b in the N(^{2}D) and P(^{2}D) states have different properties than the 2p and 3p orbitals in the N(^{4}S) and P(^{4}S) states, the bonds formed with these orbitals in the transition states will have different lengths, strengths and spatial orientations than those in the ground states.

Which lobe orbitals will be used to form bonds depends on the strength of the resulting bonds as well as the resulting interactions with the electrons in the other orbitals in the molecule. In particular, we note that the formation of bonds with the ($3s_L$, $3s_R$, $3p_y$) orbitals has a lone pair perpendicular to the yz plane that will have repulsive interactions with the lone pair orbitals in F that are also perpendicular to the yz plane. This is not the case when bonds are formed with the ($3p_L$, $3p_R$, $3p_y$) orbitals where the lone pair lies in the molecular plane.

3.2.2 GVB orbitals of the transition states

As discussed above, the ground states of the eight molecules in our study have three normal covalent bonds formed by singlet coupling the singly occupied ligand orbitals with the three singly occupied p orbitals of N(^{4}S) and P(^{4}S). Figure 5 shows the GVB bonding orbitals of the eight transition states, along with the doubly occupied lone pair orbital. When there are equivalent bonds, the GVB orbitals of only one bond are shown. The overlap between the two orbitals that form a bond is also shown. The GVB wave functions of all of the eight transition state molecules are predominantly PP spin coupled with w_{PP} ranging from 0.91 to more than 0.99.

NH_3 and PH_3 each have three equivalent bonds. Upon bond formation, the orbitals on the two atoms polarize, hybridize, expand or contract, delocalize, etc. in response to the presence of the other atoms. However, it is clear that, for instance, one of the orbitals participating in the NH bond closely resembles the 2s lobe orbital of N shown in Fig. 4, although with somewhat more 2p character than in the N atom, and the other orbital resembles the 1 s orbital of the H atom. The lone pair orbital is essentially the out-of-plane $2p_x$ orbital in the N(^{2}D) state. This is consistent with the orbital diagram 1a in Fig. 3. The three equivalent NH bonds result from resonance between the 2s-recoupled pair bond dyad and the normal covalent bond with the $2p_y$ orbital. The resulting structure has D_{3h} symmetry because this arrangement reduces the Pauli repulsion between the three bonds, and so, the GVB orbitals on the N atom in the NH_3 transition state are resonance averages (hybrids) of the two 2s lobe orbitals and the $2p_y$ orbital. The situation is similar in PH_3. The reason for the shorter bond distances in

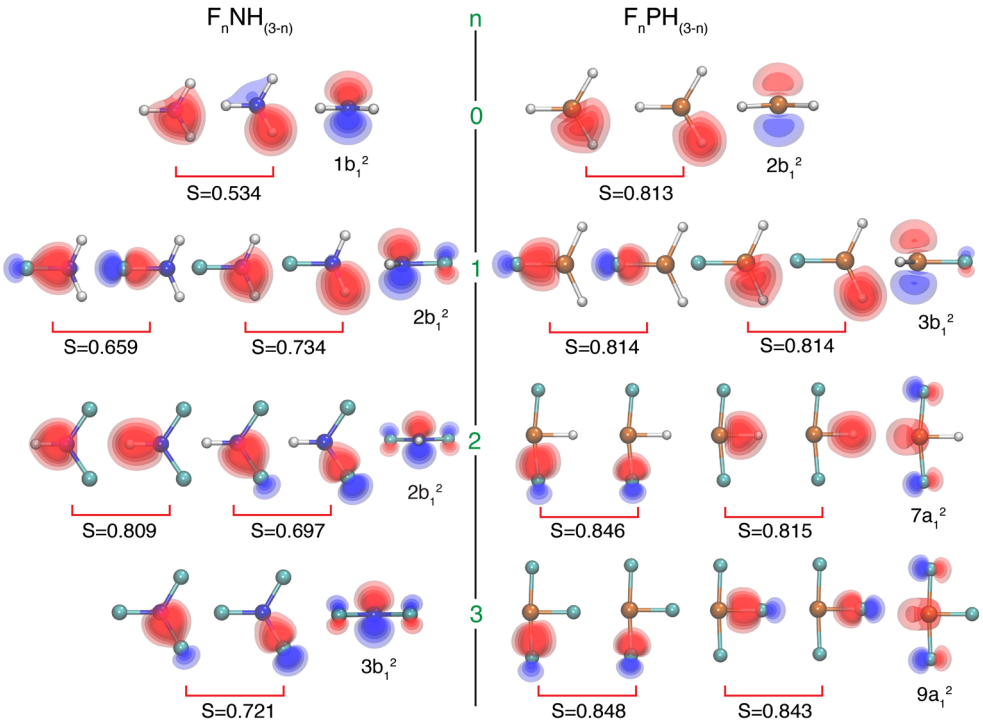

Fig. 5 Selected GVB orbitals and overlaps for the inversion transition states of $F_nNH_{(3-n)}$ and $F_nPH_{(3-n)}$ ($n = 0$–3). The GVB calculations are 6-in-6 calculations. When two or three bonds are equivalent, the two GVB orbitals constituting one bond are shown. The doubly occupied orbital on the central atom for each molecule is shown following the GVB orbitals. Contours are ±0.10, ±0.15, ±0.20 and ±0.25

the transition states is that the orbitals on N and P have large s orbital components in the transition states, and s orbitals are closer to the nucleus than p orbitals, especially for the P atom. Therefore, the bonds formed with these orbitals are shorter than those formed with p orbitals in the ground states (Question #2).

The N atom is more electronegative than the P atom, so NH bonds are more polarized toward the N atom than PH bonds. A result of this is that the three orbitals centered on N have much higher overlaps (0.782) with each other than do the three orbitals centered on P (0.442). This leads to larger Pauli repulsion between the bond pairs in NH_3. One impact of this repulsive interaction is that the H 1s-like bond orbital develops a node in the region of the N atom. As a result, the overlap of the bond pair is smaller in NH_3 (0.534) than in PH_3 (0.813).

Upon a single substitution of H by F, the geometries do not change much. But there are significant changes in some of the orbitals. The N or P orbital involved in the bond to the F atom has delocalized onto the F atom as would be expected for a polar covalent bond. This delocalization builds $N^{\delta+}F^{\delta-}$ ($P^{\delta+}F^{\delta-}$) character into the GVB wave function. The orbitals for the other two bond pairs resemble those in NH_3 and PH_3. Due to the interaction with the out-of-plane, doubly occupied $2p_x$ orbitals on F, the doubly occupied, out-of-plane $2p_x$ and $3p_x$ lone pair orbitals on N and P acquire antibonding character. Also, since F is very electronegative, the overlaps between the orbitals on the central atoms are reduced and the node in the H 1s-like orbital in NH_3 disappears upon F substitution. Regardless of these small changes, the nature of the bonding orbitals on the central atoms in FNH_2 and FPH_2 is similar to that of NH_3 and PH_3: hybrids of an s-recoupled pair bond dyad and a p-covalent bond.

Once another H atom is substituted with an F atom, there are marked differences in the geometrical and orbital structure of F_2NH and F_2PH. F_2NH is very similar to FNH_2, although two F atoms pull more electron density away from the central N atom than one F atom and the orbitals are less dense around the N atom. The overlaps between the bonding orbitals increase for both the NH and NF bonds. The out-of-plane, doubly occupied $2p_x$ orbital on N has acquired antibonding character on both F atoms, evidence of increased repulsive interactions between the electrons in the N lone pair and those in the doubly occupied $2p_x$ orbitals on F. On the other hand, F_2PH does not resemble FPH_2. The geometry of the transition state is now T-shaped, and the lone pair orbital is no longer a $3p_x$-like orbital perpendicular to the molecular plane but a 3s lobe-like orbital in the molecular plane. This latter orbital has acquired a measure of antibonding character because of the interaction of the electrons in this orbital with the doubly occupied in-plane 2p orbitals on the F atom. In addition, the orbitals participating in the axial FPF bond in the F_2PH transition state are 3p lobe orbitals instead of 3s lobe orbitals.

The two axial PF bonds in F_2PH are, in fact, a p-recoupled pair bond dyad (Question #1). The P–F bond distance is very similar to that found in the $A^2\Pi$ state of PF_2, 1.649 Å (F_2PH) versus 1.639 Å (PF_2), a molecule

known to have a p-recoupled pair bond dyad [9]. This is the reason for the unusual increase in the length of the PF axial bonds between the ground and transition state: p-recoupled pair bond dyads have bond distances that are significantly longer than the corresponding covalent bonds [9, 12, 13, 31, 40]. In contrast, the P orbital participating in the equatorial PH bond is the singly occupied 3p orbital (See 2b in Fig. 3). This bond is a normal polar covalent bond, which leads to only a slight decrease in the bond length (−0.7 % in Table 3) going from the ground state to the transition state (Question #2). Note that the p-recoupled pair bond dyad in F_2PH is almost linear, $\theta_{FPF} = 169.2°$, as suggested in the orbital diagram 2b in Fig. 3, and as the geometry of $PF_2(A^2\Pi)$ suggests ($\theta_{FPF} = 180°$). This is due to the dominant 3p character in the 3p lobe orbitals and the repulsive forces between the two PF bonds, the PH bond and the doubly occupied distorted 3s-like orbital. The quasi-linear structure is consistent with our finding that p-recoupled pair bond dyads are structurally rigid and prefer nearly collinear arrangements [9, 12, 13, 31, 40].

When all of the H atoms are substituted with F atoms, the NF_3 transition state has three equivalent NF bonds and D_{3h} symmetry. The doubly occupied orbital is an out-of-plane N $2p_x$-like orbital with antibonding character on all three F atoms. The overlap between the two bonding orbitals constituting a NF bond increases from 0.697 in F_2NH to 0.721 in NF_3 as more F atoms pull more electron density into the bonding region. PF_3 is similar to F_2PH, with the only difference being that the PH covalent bond in F_2PH becomes a PF polar covalent bond. The two axial bonds are, again, a p-recoupled pair bond dyad formed with the P 3p lobe orbitals. The axial PF bonds in PF_3 are similar in length to those in F_2PH, 1.630 Å (PF_3) versus 1.649 Å (F_2PH) and are much longer than the PF bond in the PF_3 ground state (1.567 Å). For the equatorial bond, on the other hand, the percentage change in the bond length is just −0.4 % (0.006 Å), consistent with the equatorial PF bond being a covalent bond formed with a 3p orbital. Therefore, the seemingly random bond length changes in F_2PH and PF_3 (Question #2) are, in fact, not random: The p-recoupled pair bond dyads of the transition states have much longer bond distances than the covalent bonds, and the equatorial covalent bonds of the transition states are only slightly shorter than the covalent bonds of the ground states. The doubly occupied P orbital in PF_3 is similar to that in F_2PH, a distorted 3 orbital with some antibonding character associated with the F in-plane lone pairs.

3.2.3 *Further comparison of s- and p-recoupled pair bond dyads*

The analysis of the GVB orbitals of (PH_3, FPH_2, F_2PH, PF_3) shows that the dramatic change in the structures of the transition states for F_2PH and PF_3 is a result of the formation of a p-recoupled pair bond dyad in these species (Question #1). In this section, we take a step back to examine the triatomic molecules, because recoupled pair bond dyads also exist in NH_2, NF_2, PH_2 and PF_2, although in their excited states not in their ground states. Here, we focus on PH_2 and PF_2 as two examples of s- and p-recoupled pair bond dyads.

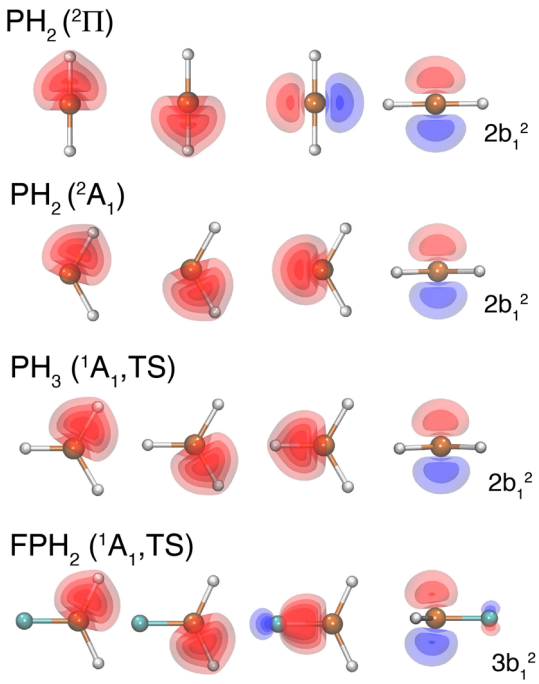

Fig. 6 GVB orbitals centered on the P atom for the linear $PH_2(^2\Pi)$ configuration, the bent $PH_2(^2A_1)$ excited state, and for the transition states for inversion in $FPH_2(^1A_1)$ and $PH_3(^1A_1)$

The ground state of PH_2 is a $^2B_1$ state, bound by two normal covalent bonds. The first excited state is a $^2A_1$ state. The $^2A_1$ state derives from a linear $^2\Pi$ state that contains a 3s-recoupled pair bond dyad, and relaxes to a bent geometry upon geometry optimization, incorporating additional 3p character into the P bonding orbitals. So let us compare the recoupled pair bond dyad in the $^2\Pi$ and $^2A_1$ states of PH_2 with the bonds in the PH_3 and FPH_2 transition states to understand how the s-recoupled pair bond dyad evolves in these species. Figure 6 shows the GVB orbitals in PH_2, PH_3 and FPH_2 that are centered on the P atom along with the doubly occupied, out-of-plane 3p-like lone pair orbitals. The $PH_2(^2\Pi)$ state has two 3s-like lobe orbitals as well as singly and doubly occupied 3p(π)-like orbital on the P atom. The 3s lobe orbitals are slightly delocalized onto the H atoms compared to the 3s lobe orbitals in the P atom (Fig. 4). In order to strengthen the bond and reduce the repulsion between the electrons in these orbitals and because mixing between (hybridization of) s and p orbitals is facile, the $^2\Pi$ state rearranges to become a strongly bent

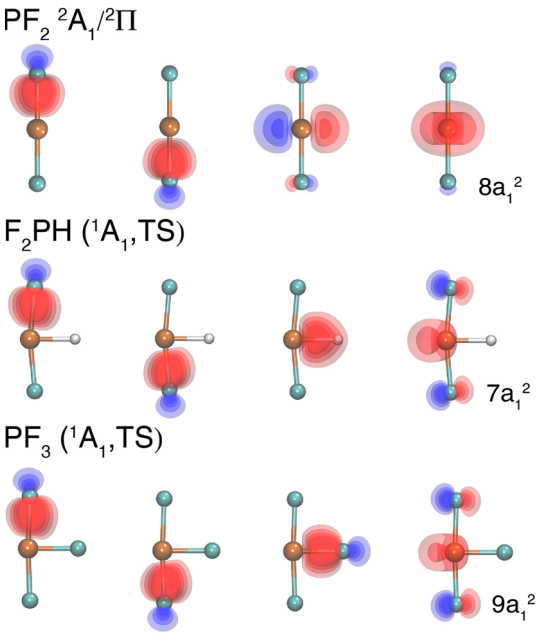

Fig. 7 GVB orbitals centered on the P atom for the linear $PF_2(^2\Pi)$ excited state and the transition states for $F_2PH(^1A_1)$ and $PF_3(^1A_1)$

$^2A_1$ state with a bond angle of 121.8°, reducing the energy by 19.66 kcal/mol. The 3p orbital is pushed away from the two PH bonds, picking up 3s character. So the three singly occupied P orbitals in the $^2A_1$ state of PH_2 are not pure 3s lobe orbitals or 3p orbitals, but a mixture of the two. However, their origins are clear.

The singly occupied P orbitals in the PH_3 transition state look very much like the corresponding orbitals in the $PH_2(^2A_1)$ state. The doubly occupied out-of-plane orbital is largely unchanged. The orbitals of the FPH_2 transition state are similar except that the P bonding orbital delocalizes onto the F atom (consistent with the fact that the F atom is more electronegative than the P atom), and the out-of-plane lone pair orbital acquires antibonding character due to repulsive interactions of the electrons in this orbital with those in the F 2p orbital.

Similar comparisons for PF_2, F_2PH and PF_3 are given in Fig. 7. The ground state of PF_2 is also a $^2B_1$ state, and the lowest-lying excited state is a $^2\Pi$ state. In PF_2, in contrast to PH_2, the first excited state is linear. The $PF_2(^2\Pi)$ state contains a 3p-recoupled pair bond dyad, a singly occupied 3p-like orbital and a doubly occupied polarized 3s lone pair orbital ($8a_1$) [9]. As noted previously, p-recoupled pair bonds prefer linear or quasi-linear geometries [9, 12, 13, 31, 40]. Comparing the three molecules containing the p-recoupled pair bond dyad, one can see that the 3p-like lobe orbitals remain largely unchanged. The biggest changes occur for the 3p-like orbital and the doubly occupied 3s-like orbital as the third bond forms in F_2PH and F_2PF. The 3p-like P orbital localizes in the bonding region as the PH bond forms and then delocalizes onto the more electronegative F atom when the PF bond forms. The 3s-like orbitals gain antibonding character and are pushed away from the covalent bonds. Comparing Figs. 6 and 7, one can see the s-recoupled pair bond dyad is indeed much more structurally flexible than the p-recoupled pair bond dyad.

As shown above, it is possible for the same central atom to form different types of recoupled pair bonds and recoupled pair bond dyads. As shown in Fig. 4, the overlap between the $3s_L$ and $3s_R$ lobe orbitals of the P atom is 0.776, while the overlap between $3p_L$ and $3p_R$ is 0.839. Therefore, it is much easier to form an s-recoupled pair bond than a p-recoupled pair bond. In fact, forming a p-recoupled pair bond dyad requires electronegative ligands, which separates the two highly overlapping p lobe orbitals and reduces the Pauli repulsion between the resulting bond pairs [31]. The H atom is not sufficiently electronegative to recouple the P $3p^2$ lone pair. Therefore, the $P(^2D)$ state forms an s-recoupled pair bond dyad with two H atoms and a p-recoupled pair bond dyad with two F atoms. Although the F atom is also able to recouple a $3s^2$ lone pair, an s-recoupled pair bond dyad does not form in F_2PH and PF_3 because the P lone pair orbital would then be perpendicular to the molecular plane, resulting in strong Pauli repulsive interactions with the electrons in the doubly occupied orbitals on the F atoms. These repulsions are minimized if the lone pair on the P atom is in a 3s-like orbital, which is polarized away from the F atoms as is the case for the p-recoupled pair bond dyad. Therefore, the p-recoupled pair bond dyad is preferred, which gives rise to the low-barrier inversion pathways in F_2PH and PF_3 (Question #3). Even though the lone pair on the P atom is not involved in bond formation, it clearly influences which types of bonds are formed.

3.3 Transition state formation pathways

To summarize the above GVB analysis of the transition states, GVB diagrams of the pathways for forming the inversion transition states of two representative molecules, NF_3 and PF_3, are shown in Fig. 8. The NF_3 transition state goes through a pathway involving the formation of an s-recoupled pair bond dyad. The two F atoms recouple the $2s^2$ electrons of $N(^2D)$ and form the $NF_2(^2\Pi)$ configuration, which rearranges to the bent $^2A_1$ state. The third F atom forms a normal (polar) covalent bond with the singly occupied orbital in the $NF_2(^2A_1)$ state, leading to the NF_3 D_{3h} transition state. The doubly occupied orbital on N is perpendicular to the molecular plane. The three NF bonds are equivalent as a result of the ease with which s and p orbitals hybridize (mix). The very high barrier to inversion in NF_3 is, in large part, due to the strong repulsions between the electrons in the lone pair orbital on the N atom and those in the lone pair orbitals on the F atom.

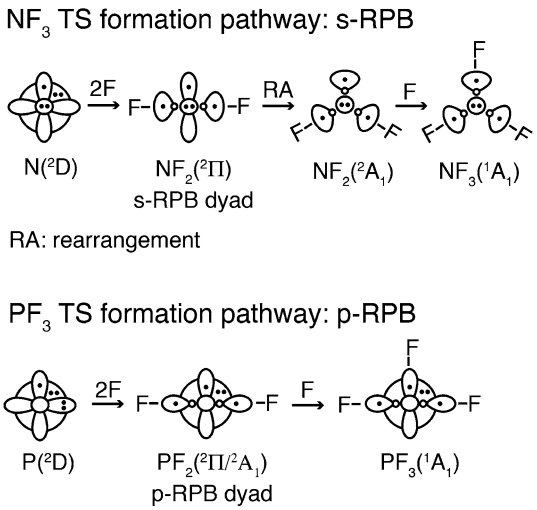

Fig. 8 Formation pathway diagrams of the $^1A_1$ inversion transition states for NF_3 and PF_3

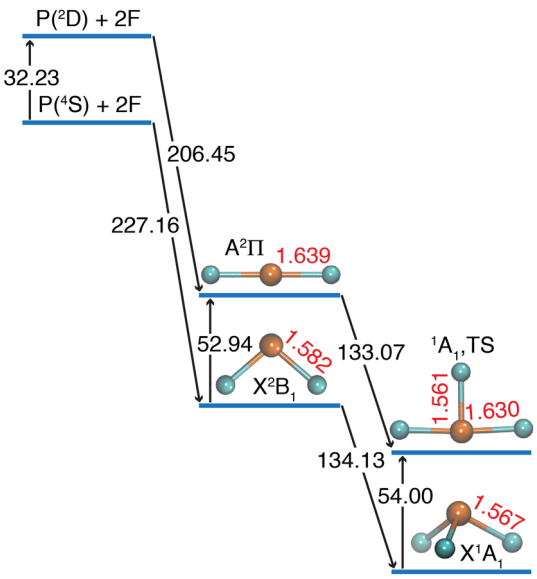

Fig. 9 Energy and bond length changes during the formation of the ground state and inversion transition state of PF_3, beginning with the atoms. The energies are in kcal/mol, and bond distances are in Å

The PF_3 transition state goes through a p-recoupled pair bond dyad pathway. The two F atoms recouple the $3p^2$ electrons of $P(^2D)$ to form the $PF_2(^2\Pi)$ state. The third F atom then forms a normal covalent bond with the remaining singly occupied P 3p orbital, resulting in a T-shape transition state structure. The lone pair orbital on P in PF_3 is a distorted 3s-like orbital polarized away from the F atoms in order to reduce the repulsions between the electrons in this orbital and those in the F lone pair orbitals. The collinear structure of the p-recoupled pair bond dyad remains almost unchanged in the process, with the dyad bonds bending slightly away from the lone pair. Not only are the axial bond lengths nearly the same in $PF_2(A^2\Pi)$ and $PF_3(^1A_1$, TS), but the F_2P–F ground and transition state bond energies are nearly the same, which means that the magnitude of the inversion barrier is nearly the same as the energy difference between the $PF_2(X^2B_1)$ and $PF_2(A^2\Pi)$ states, 54.00 versus 52.94 kcal/mol. This process is illustrated in Fig. 9. The bond energy of the equatorial PF bond in the transition state is 133.07 kcal/mol (the bond energy reported in ref. [9] is incorrect), similar to the 134.13 kcal/mol bond energy of the covalent PF bond in the ground state. Also, the energy lowering for forming a p-recoupled pair bond dyad from the atoms in $PF_2(A^2\Pi)$ is 206.45 kcal/mol, which is only 20.71 kcal/mol less stable than forming the two covalent bonds in $PF_2(X^2B_1)$, 227.16 kcal/mol. In fact, as noted earlier, the strength of recoupled pair bond dyads is the reason for the existence of hypervalent species such as PF_5 [9] and SF_6 [12].

4 Conclusions

In this article, we report accurate CCSD(T) calculations on the ground and transition states for inversion of the $F_nNH_{(3-n)}$ and $F_nPH_{(3-n)}$ ($n = 0$–3) molecules along with a detailed analysis of the GVB wave functions for these molecules at the calculated stationary points. All of the molecules go through D_{3h}-like transition states, except for PF_3 and F_2PH, which have T-shaped transition states, a fact first reported by Dixon and coworkers [4–8]. For all of the molecules with D_{3h}-like transition states, the bond distances are shorter than those in their ground states, a result of the increased s character in the N and P bond orbitals in the transition states. However, for F_2PH and F_2PF, the transition state is T-shaped and the axial PF bonds are much longer than those in the ground state, while the equatorial PH and PF bonds are slightly shorter than those in the F_2PH and PF_3 ground states.

Likewise, there is a dramatic difference in the dependence of the barrier height for inversion as the number of F atoms (n) increases. The height of the inversion barrier height increases dramatically for the $F_nNH_{(3-n)}$ series as n increases, from 5.34 (NH_3) to 82.79 (NF_3) kcal/mol. However, for the $F_nPH_{(3-n)}$ series, the barrier height increases substantially from $n = 0$ to $n = 1$ (33.25–50.54 kcal/mol), but thereafter it increases only modestly (from 50.54 to 54.00 kcal/mol).

The explanation for the anomalous behavior of the F_2PH and PF_3 molecules is simple. In the transition states of both F_2PH and PF_3, the nearly collinear PF bonds are a result of the formation of p-recoupled pair bond dyads. A hydrogen atom is not sufficiently electronegative to recouple the lone pair in the $P(^2D)$ excited state, and therefore, these bonds are only found in F_2PH and PF_3. Formation of the p-recoupled pair bond dyads in the transition states of these two

molecules is favored because it minimizes the repulsion between the electrons in the lone pair on P and those in the lone pairs on the F atoms. Since a p-recoupled pair bond dyad prefers a nearly collinear arrangement of the F–P-F atoms, the transition states in F_2PH and PF_3 are T-shaped. The lengthening of the axial PF bonds is a result of the formation of p-recoupled pair bond dyads in F_2PH and PF_3, while the third bond in each species is a covalent bond similar to that in the ground state.

The ground state of F_2PH and PF_3 arises from the addition of an H or F atom to the ground state of PF_2, the X^2B_1 state, while the T-shaped transition arises from the corresponding additions to the first excited state of PF_2, the $A^2\Pi$ state. The energy of the $PF_2(X^2B_1)$ and $PF_2(A^2\Pi)$ states differs by 52.94 kcal/mol [9]. If the strengths of the PH and PF bonds in the F_2PH and PF_3 transitions states are similar to those in the ground states, as would be expected, one would predict barrier heights close to this value, which, indeed, is the case: 52.04 kcal/mol (F_2PH) and 54.00 kcal/mol (PF_3). In addition, it should be noted that the lengths of the covalent PH and PF bonds are similar in the ground and transition states.

In summary, the transition states for NH_3, FNH_2, F_2NH, NF_3, PH_3 and FPH_2 involve the formation of s-recoupled pair bond dyads. Neither the H or F atoms are able to recouple the $2p^2$ lone pair in the $N(^2D)$ state, so all of the transition states in the $F_nNH_{(3-n)}$ series possess s-recoupled pair bond dyads (or hybrids thereof). H is not able to recouple the $3p^2$ lone pair of P atom, and thus, the PH_3 and FPH_2 transition states also contain s-recoupled pair bond dyads. Extensive mixing between the s-recoupled pair bond dyad and the remaining covalent bond results in the D_{3h}-like transition state structures and vertex inversion pathways. The F atom is sufficiently electronegative to recouple both the $3s^2$ and the $3p^2$ electrons of the P atom, but the p-recoupled pair bond dyad is preferred in F_2PH and PF_3 over the s-recoupled pair bond dyad because the repulsion between the out-of-plane lone pair on P and the lone pairs on F is smaller in the former case. This leads to much lower inversion barriers than expected for F_2PH and PF_3 based on the trends in the $F_nNH_{(3-n)}$ and the first two members of the $F_nPH_{(3-n)}$ series. The p-recoupled pair bond dyad is rigid and stays almost collinear when other bonds are formed, which results in the T-shaped transition states and edge inversion in F_2PH and PF_3.

The T-shaped pnictogen structures in the ground state and transition states of compounds such as ADPO and its saturated analog also result from the formation of p-recoupled pair bond dyads by the pnictogen elements from the second row and beyond. Factors that stabilize the T-shaped structures of these compounds include electronegative ligands (facilitating the formation of the recoupled pair bond dyad) and conjugated π system (allowing delocalization into the space usually occupied by the lone pair). Such compounds are expected to be widespread; their chemistry has been reviewed in detail by Arduengo and Stewart [2].

Acknowledgments This work was supported by funding from the Distinguished Chair for Research Excellence in Chemistry and the National Center for Supercomputing Applications at the University of Illinois at Urbana-Champaign.

References

1. Culley SA, Arduengo AJ III (1984) J Am Chem Soc 106:1164–1165
2. Arduengo AJ III, Stewart CA (1994) Chem Rev 94:1215–1237
3. Lochschmidt S, Schmidtpeter A (1985) Z Naturforsch Teil B 40:765–773
4. Dixon DA, Arduengo AJ III, Fukunaga T (1986) J Am Chem Soc 108:2461–2462
5. Arduengo AJ III, Dixon DA, Roe DC (1986) J Am Chem Scc 108:6821–6823
6. Dixon DA, Arduengo AJ III (1987) J Chem Soc Chem Comm 2:498–500
7. Dixon DA, Arduengo AJ III (1987) J Am Chem Soc 109:338–341
8. Dixon DA, Arduengo AJ III, Lappert M (1991) Heteroatom 2:541–544
9. Woon DE, Dunning TH Jr (2010) J Phys Chem A 114:8845–8851
10. Clotet A, Rubio J, Illas F (1988) J Mol Struc (Theochem) 164:351–361
11. Creve S, Nguyen MT (1998) J Phys Chem A 102:6549–6557
12. Woon DE, Dunning TH Jr (2009) J Phys Chem A 113:7915–7926
13. Chen L, Woon DE, Dunning TH Jr (2009) J Phys Chem A 113:12645–12654
14. Purvis GD III, Bartlett RJ (1982) J Chem Phys 76:1910–1918
15. Raghavachari K, Trucks GW, Pople JA, Head-Gordon M (1989) Chem Phys Lett 157:479–483
16. Knowles PJ, Hampel C, Werner HJ (1993) J Chem Phys 99:5219–5227
17. Watts JD, Gauss J, Bartlett RJ (1993) J Chem Phys 98:8718–8733
18. Dunning TH Jr (1989) J Chem Phys 90:1007–1023
19. Kendall RA, Dunning TH Jr, Harrison RJ (1992) J Chem Phys 96:6796–6806
20. Woon DE, Dunning TH Jr (1993) J Chem Phys 98:1358–1371
21. Dunning TH Jr, Peterson KA, Wilson AK (2001) J Chem Phys 114:9244–9253
22. Goddard WA III, Blint RJ (1972) Chem Phys Lett 14:616–622
23. Goddard WA III, Dunning TH Jr, Hunt WJ, Hay PJ (1973) Acc Chem Res 6:368–376
24. MOLPRO is a package of ab initio programs written by Werner HJ, Knowles PJ, Knizia G, Manby FR, Schütz M, Celani P, Korona T, Lindh R, Mitrushenkov A, Rauhut G, Shamasundar KR, Adler TB, Amos RD, Bernhardsson A, Berning A, Cooper DL, Deegan MJO, Dobbyn AJ, Eckert F, Goll E, Hampel C, Hesselmann A, Hetzer G, Hrenar T, Jansen G, Köppl C, Liu Y, Lloyd AW, Mata RA, May AJ, McNicholas SJ, Meyer W, Mura ME, Nicklaß A, O'Neill DP, Palmieri P, Peng D, Pflüger K, Pitzer R, Reiher M, Shiozaki T, Stoll H, Stone AJ, Tarroni R, Thorsteinsson T, Wang M. See http://www.molpro.net

25. Knowles PJ, Werner HJ (1985) Chem Phys Lett 115:259–267
26. Werner HJ, Knowles PJ (1985) J Chem Phys 82:5053–5063
27. Knowles PJ, Werner HJ (1988) Chem Phys Lett 145:514–522
28. Werner HJ, Knowles PJ (1988) J Chem Phys 89:5803–5814
29. Ragavachari K, Trucks GW, Pople JA, Head-Gordon M (1989) Chem Phys Lett 157:479–483
30. Langhoff SR, Davidson ER (1974) Int J Quant Chem 8:61–72
31. Dunning TH Jr, Woon DE, Leiding J, Chen L (2013) Acc Chem Res 46:359–368
32. Lindquist BA, Woon DE, Dunning TH Jr (2014) J Phys Chem A 118:1267–1275
33. Woon DE, Dunning TH Jr, to be published
34. Gerratt J, Cooper DL, Karadakov PB, Raimondi M (1997) Chem Soc Rev 26:87–100 and references therein
35. Cooper DL, Thorsteinsson T, Gerratt J (1997) Int J Quant Chem 65:439–451
36. Thorsteinsson T, Cooper DL (1998) Int J Quant Chem 70:637–660
37. Cooper DL, Thorsteinsson T, Gerratt J (1998) Adv Quant Chem 32:51–67
38. Cooper DL, Karadakov PB (2009) Int Rev Phys Chem 28:169–206
39. NIST Atomic Spectra Database (ver. 5.1), [Online]. Available at: http://physics.nist.gov/asd [2014, February 2]
40. Leiding J, Woon DE, Dunning TH Jr (2011) J Phys Chem A 115:4757–4764